Atlantic Multidecadal Variability in a model with an improved North Atlantic Current

Annika Drews[1] and Richard J. Greatbatch[1,2]

Corresponding author: A. Drews, GEOMAR Helmholtz-Zentrum für Ozeanforschung Kiel, Düsternbrooker Weg 20, 24105 Kiel, Germany. (adrews@geomar.de)

[1]GEOMAR Helmholtz Centre for Ocean Research Kiel, Kiel, Germany.

[2]Faculty of Mathematics and Natural Sciences, University of Kiel, Kiel, Germany.

Key Points.

- Simulated AMV is improved in a model with a realistic North Atlantic Current
- Ocean controls AMV in the northwestern part, atmosphere transfers heat to eastern and southern parts
- Atmosphere/ocean heat transfer is modified on interdecadal time scales by the atmosphere

We examine the simulated Atlantic Multidecadal Variability (AMV) in a model that includes a correction for a longstanding problem with climate models, namely the misplacement of the North Atlantic Current. The corrected model shows that in the warm AMV phase, heat is lost by the ocean in the northwestern part of the basin and gained by the ocean to the east, suggesting an advective transfer of heat by the mid-latitude westerlies. The basin wide response is consistent with a role for cloud feedback and is in broad agreement with estimates from observations, but is poorly represented in the uncorrected model. The corrected model is then used to show that the ocean/atmosphere

heat transfer is influenced by low frequency variability in the overlying atmosphere. We also argue that changing ocean heat transport is an essential feature of our results.

1. Introduction

North Atlantic sea surface temperatures (SSTs) exhibit pronounced basin scale variability on multidecadal time scales. This mode of coherent warming/cooling is known as the Atlantic Multidecadal Variability [AMV; *Schlesinger and Ramankutty*, 1994; *Enfield et al.*, 2001; *Sutton and Hodson*, 2005; *Knight et al.*, 2005; *Dima and Lohmann*, 2007]. The time series and spatial pattern of the AMV based on observations are shown in Figures 1a and 2a (see Section 3 for the precise definition of the AMV). The former shows pronounced multidecadal variability while the latter exhibits a basin-wide SST signature with a maximum east of Newfoundland and a weaker signature in the subtropics.

The AMV has been shown to influence North American and European Summer climate [*Sutton and Hodson*, 2005], US rainfall [*Enfield et al.*, 2001] and drought [*McCabe et al.*, 2004], Sahel rainfall [*Folland et al.*, 1986], Atlantic hurricanes [*Goldenberg et al.*, 2001], the Indian monsoon [*Zhang and Delworth*, 2006], South American rainfall [*Kayano and Capistrano*, 2014], Arctic temperature change [*Chylek et al.*, 2009], and temperature over the whole Northern Hemisphere [*Steinman et al.*, 2015], to name but a few studies. Through its impact, the AMV is of great socio-economic relevance. Therefore, it is highly desirable to understand its dynamics and potential predictability.

The dynamics of the AMV are under debate. It has long been thought that the Atlantic Meridional Overturning Circulation (AMOC) plays an important role, with a stronger (weaker) AMOC enhancing (reducing) the North Atlantic heat content, of which the AMV is the surface imprint in this paradigm [e.g., *Latif et al.*, 2004; *Knight et al.*, 2005; *Latif and Keenlyside*, 2011; *McCarthy et al.*, 2015]. Some studies, however, have suggested

that the AMV is largely driven by changing radiative forcing, e.g., from volcanoes [*Otterå et al.*, 2010]. *Booth et al.* [2012] go further and argue that variations in aerosol loading are a key factor, a view that has been criticized by *Zhang et al.* [2013]. The mixture of free and forced variability complicates the interpretation of both models and observations, with both forms of variability likely to play a role in reality [*Tandon and Kushner*, 2015]. Even the nature of the free variability is not without controversy. In particular, *Clement et al.* [2015] claim that the AMV is entirely driven by fluxes from the atmosphere, with no role for the AMOC and the associated heat transport variations, a view that has been challenged by, e.g., *O'Reilly et al.* [2016].

Aside from the role of variable radiative forcing, a further complication when interpreting models is the cold SST bias in the North Atlantic that is a common feature of climate models and is associated with the southward displacement of the North Atlantic Current in the models [Fig. S1 in the supporting information; *Wang et al.*, 2014; *Flato et al.*, 2014; *Drews et al.*, 2015; *Menary et al.*, 2015]. Different climate models simulate AMV patterns that are distorted and/or shifted from observed estimates and from each other [*Ba et al.*, 2014; *Brown et al.*, 2016]. Here, we show the advantage of using a flow field correction, as described in *Drews et al.* [2015], to alleviate the cold SST bias in a coupled model. Our bias corrected model shows a much more realistic representation of the AMV than does the uncorrected model and throws light on the role of the atmosphere for setting the basin wide character of the AMV. In addition, we show that the AMV in our model cannot be reproduced without having a dynamic ocean and the associated AMOC variations, addressing the issue raised by *Clement et al.* [2015]. We also show that

the relationship between the air-sea heat exchange and the AMV can be modulated by low frequency variability in the atmosphere. For example, *Yamamoto and Palter* [2016] have argued that the absence of an AMV fingerprint in the observed record of winter mean European surface air temperature is because of the tendency, along air parcel trajectories, for more heat to be removed from the North Atlantic in the cold than in the warm phase of the AMV during the observed record in winter, a feature we can address with our model set-up.

2. Data and Methods

2.1. The coupled model and the flow field correction

For this study, we use the Kiel Climate Model [KCM; *Park et al.*, 2009], a coupled atmosphere/ocean/sea ice model. It consists of the ocean model NEMO [*Madec*, 2008] in the ORCA2 configuration ($\approx 2^\circ \times 2^\circ$, 31 vertical levels) coupled to the atmospheric model ECHAM5 [*Roeckner et al.*, 2003] with approximately $3.75^\circ \times 3.75^\circ$ resolution (T31), 19 vertical levels and a lid at 10hPa, using the coupler OASIS3 [*Valcke*, 2006, 2013]. The radiative forcing is fixed at late twentieth century levels and, in particular, does not include changing greenhouse gas concentration or aerosol loading.

We compare model output of the KCM run in the standard configuration (hereafter "the uncorrected model" or "CTRL") with output from a corrected model version (referred to as "CORR"). CORR includes a non-flow interactive correction that is applied to the North Atlantic flow field as well as an additional correction that is applied to the surface freshwater flux (model experiment C-FS0 as described in *Drews et al.* [2015]). The flow field correction adjusts the baroclinic pressure gradient of the ocean component by a non-

interactive seasonally varying climatological correction term in the momentum equations. The correction leads to a more northward flow of the North Atlantic Current (NAC), re-establishing the northwest corner [*Lazier*, 1994] east of Newfoundland (see Fig. S2). In order to prevent a shutdown of the AMOC, the surface freshwater flux seen by the ocean component is also adjusted. However, no adjustment is made to the model heat budget. Further details can be found in *Drews et al.* [2015]. 1000 year long model simulations are carried out using both model versions and the last 700 years, annually averaged (unless otherwise stated) and, here, 5 year low pass filtered, are analyzed.

2.2. Gridded Observational Data Sets

We compare our model results with SST from the Hadley Centre sea Ice and Sea Surface Temperature data set (HadISST, from 1900 to 2012) [*Rayner et al.*, 2003] and turbulent, i.e., sensible and latent, heat flux data produced by *Gulev et al.* [2013], available from 20° – 70° N in the North Atlantic.

3. Results

We define the AMV as the linearly detrended area mean North Atlantic SST between the equator and 60° N, 75° W and 7.5° W [*Sutton and Hodson*, 2005; *Ting et al.*, 2009], annually averaged and, here, 5 year low pass filtered. CTRL simulates variability analogous to the observed AMV, albeit with lower amplitude and shorter time scale (Figs. 1b and S3 and note the dominance of decadal rather than multidecadal variability in this model version[1]), an aspect of the model performance that is improved in CORR (Fig. 1c). In observations, the region of maximum SST variability is found in the northwest corner region (Fig. 2a), just to the east of Newfoundland, whereas in CTRL, it is shifted

to the south and east (Fig. 2b). This is perhaps not surprising given the southeastward displacement of the North Atlantic Current and the lack of a northwest corner in CTRL [*Drews et al.*, 2015, see Fig. S1 and S2]. Correcting the flow field moves the North Atlantic Current to a more realistic location [*Drews et al.*, 2015] and leads to a more realistic pattern of SST variability associated with the AMV (Fig. 2c). The SST variability is now at a maximum in the northwestern part of the North Atlantic, south of Greenland, in a region where CTRL shows, by contrast, a local minimum in SST variability. On the other hand, the variability in the deep tropics is less pronounced in CORR than in the pattern derived from observations, with the characteristic horseshoe pattern bending westwards further north than in observations. There is evidence that cloud feedback is important for the tropical signature of the AMV [*Brown et al.*, 2016; *Yuan et al.*, 2016], a process that appears to operate in our model but probably not sufficiently in the deep tropics. Nevertheless, the pattern of SST variability derived from CORR is quite similar to the ensemble mean from the CMIP5 simulations shown in Figure 1a of *Brown et al.* [2016]. By contrast, the SST pattern derived from individual models shown in Figure S2 of *Brown et al.* [2016] varies considerably from model to model and sometimes shows features similar to those in CTRL (e.g., the MPI-ESM-MR model).

Examining the interaction of the ocean and the atmosphere associated with the AMV in CORR reveals an anomalous warming of the atmosphere by the ocean in the warm phase of the AMV in the northwestern part of the basin, while the atmosphere gives anomalous heat back to the ocean in the eastern and, to a lesser extent, parts of the tropics, thereby leading to a basin-wide warming (see Fig. 3b; heat flux is defined as positive upward).

Although there is the suggestion of this pattern in CTRL (Fig. 3a), the pattern is clearly distorted by the presence of the cold bias, especially in the subpolar gyre. This pattern, in which anomalous heat is given up by the ocean in the northwest and given back to the ocean in the east and the tropics, has been noted by *Brown et al.* [2016]. These authors show that cloud feedback plays an important role in models, both for amplifying the AMV signal in the northwestern Atlantic and for transferring heat from the atmosphere to the ocean in the tropical regions. We can see this effect in our model when using the total net heat flux for the regression (see Fig. S4) instead of only the sensible and latent heat flux used in Fig. 3b. In particular, Fig. S4 shows some amplification of the regression pattern in the subpolar North Atlantic as well as a region of quite pronounced heat input in the tropics that is not so clear from Fig. 3b. Since the difference between the sensible and latent heat flux and the net heat flux is dominated by the short wave component, this is consistent with a role for cloud feedback in our model. The region of heat uptake by the ocean to the west of Europe is, nevertheless, also found in the model version without cloud feedback discussed by *Brown et al.* [2016, see their Fig. 4e]. We suggest that this region of heat uptake is associated with the advection of heat from the northwestern part of the basin by the mid-latitude westerly winds, a process that may also play a role in more tropical latitudes due to advection around the subtropical (Azores) anticyclone. Advection of heat by the westerly winds in the atmosphere has been discussed by *Yamamoto and Palter* [2016] as a mechanism by which the AMV influences European climate. It is also interesting to note that the subsurface ($200 - 880$ m) heat content in CORR regressed on the AMV index with zero lag (not shown) does not show

the contrast between the western and eastern sides of the subpolar gyre that one sees in the surface heat flux. However, going along with the subsurface heat content anomalies, the subpolar gyre transport is reduced in the warm phase of the AMV (see Figure S5), favouring heat transport convergence in the ocean on the western side of the subpolar gyre at the expense of the eastern side, an issue we shall explore further elsewhere. We also note, as for SST, the similarity between the pattern of the AMV-related net surface heat flux in CORR (Fig. S4) and that from the ensemble mean of the CMIP5 models shown in *Brown et al.* [2016, see their Fig. 1b], albeit with some differences in detail (in CORR, the regression coefficient is higher and the region of strongest heat release to the atmosphere is more confined to the western North Atlantic). On the other hand, individual models (see Figure S3 from *Brown et al.* [2016]) often show very different patterns that are sometimes quite similar to that from CTRL (e.g., GFDL-ESM2M or the MPI-ESM-MR).

We turn now to an estimate of the AMV-related surface turbulent heat flux based on observations. Figure 3c shows the same regression but this time using the annual mean AMV from observations (HadISST) and surface sensible and latent heat fluxes from the data set produced by *Gulev et al.* [2013]. Here, we smoothed the data with an 11 year running mean filter as in the original article (it should be noted that applying an 11 year running mean to the model output does not qualitatively affect the comparison - see Fig. S6). It is clear that the pattern derived from observations is much closer to the pattern derived from CORR than to that derived from CTRL. A notable area of agreement is the region in the northwestern Atlantic where, in the warm phase, heat is given up by the ocean to the atmosphere. This region is almost coincident spatially in both CORR and in

the observed estimate and is of similar magnitude in both cases. The main discrepancy is the region close to Greenland and in the Labrador Sea where heat is taken up by the ocean from the atmosphere in the observed estimate and which is not found in CORR. However, in this region, the observed estimate does not pass the significance test and is probably also compromised by sparse data. Nevertheless, the difference could reflect model deficiencies, in particular the lack of resolution to properly resolve the shelf/slope circulation, especially the Labrador Current along the shelf break, and the fact that in the Labrador Sea there is still too much sea ice in CORR (cf. masked areas in Fig. 2a and c).

A difficulty when interpreting surface fluxes associated with the AMV derived from observations is the shortness of the record. *Yamamoto and Palter* [2016] have argued that the absence of an AMV signal in European winter mean surface air temperature is because of the tendency for "swifter, more zonal winds" in negative (cold) AMV winters compared to positive (warm) AMV winters. As noted by *Yamamoto and Palter* [2016], this is similar to the behaviour associated with the winter North Atlantic Oscillation (NAO) [*Hurrell*, 1995], for which positive NAO winters are associated with stronger zonal winds than negative NAO winters. Given such a relationship between the zonal winds and the AMV, *Yamamoto and Palter* [2016] argue that more heat is removed from those parts of the North Atlantic that matter for European winter climate in the cold phase than in the warm phase of the AMV, thereby masking the AMV signal over Europe. We can illustrate this effect using CORR by looking for an episode in which the winter AMV and NAO are negatively correlated (using 5 year low pass filtered time series). In CORR, the

winter (December-January-February, DJF) NAO has no correlation with the winter AMV at the 0 lag. However, a particular 70 year episode in the 1000 year long model simulation was found and analyzed (years 620-689 - see Figure 1), which shows an anti-correlated NAO–AMV relationship ($r = -0.53$ at zero lag, a very rare event in this model run). During these 70 model years (see Figure 4a), the regression of winter (DJF) turbulent surface heat fluxes on the winter (DJF) AMV index looks quite different from that shown in Fig. 3b. In particular, more heat is lost to the atmosphere during the cold phase than in a warm phase of the AMV over large parts of the subpolar North Atlantic, leading to a pattern not dissimilar to that shown in Fig. 3e of *Yamamoto and Palter* [2016]. However, when considering all winters from the 700 year time series (Fig. 4b), the pattern looks very similar that in Fig. 3b.

Finally, we note that when a 50 meter deep slab ocean without any ocean circulation is forced with the turbulent (i.e., sensible and latent) monthly mean heat flux anomalies from CORR (details in the supporting information), the spatial pattern found when regressing the slab ocean SSTs on the slab ocean AMV index (Fig. S7a) is similar to that in CORR (Fig. 2c). However, the pattern of the surface heat fluxes associated with the slab ocean AMV index (Fig. S7b) is reversed compared to that of CORR (Fig. 3b; see also Fig. 1c in *O'Reilly et al.* [2016]). In other words, the slab ocean AMV index has an 180° offset compared to the coupled model AMV index (see Fig. S8), despite being driven by the time series of surface heat fluxes from the coupled model. It follows that the mechanism driving the AMV in the fully coupled model is quite different from that in the slab ocean model, the warm phase of the AMV in the coupled model corresponding to the cold phase

of the AMV in the slab model, pointing to the fundamental role being played in the coupled model by the variations in ocean heat transport that are missing from the slab model. The results confirm those found by *O'Reilly et al.* [2016] concerning the role of changing ocean heat transport in the dynamics of the AMV in coupled models. It should be noted, too, that in CORR, the AMV and the AMOC at 48° N, 1400m depth, are highly correlated with $r \approx 0.6$ at 0 to 3 years lag (AMOC leading the AMV, both time series detrended and 5 year low pass filtered), significantly different from zero at the 99 % level using the method of *Ebisuzaki* [1997] and not sensitive to the choice of AMOC index. This underlines the strong relationship between the AMV and the AMOC in CORR.

4. Summary and Conclusions

A correct simulation of the Atlantic Multidecadal Variability (AMV) is important given the known impact of the AMV on the weather and climate of the Northern Hemisphere (see, for example, *Folland et al.* [1986]; *Goldenberg et al.* [2001]; *Knight et al.* [2005]; *Sutton and Hodson* [2005]; *Zhang and Delworth* [2006]; *Steinman et al.* [2015]). However, a common feature of coupled climate models is the misplacement of the North Atlantic Current and the associated North Atlantic cold bias [*Wang et al.*, 2014; *Drews et al.*, 2015]. Here, we have looked at the impact of the bias on the representation of the unforced AMV using two versions of the Kiel Climate Model (KCM), one of which includes a correction for the bias, following *Drews et al.* [2015], and one of which does not. A novel feature of the correction technique is the use of a flow field correction that is applied to the model momentum equations and adjusts the North Atlantic Current to a more realistic location than in the uncorrected model, CTRL. Neither model version includes changing

greenhouse gas forcing or aerosol loading and it should be noted that the correction technique does not involve adjusting the model heat budget.

We have shown that the representation of the AMV is much improved in the corrected model, CORR, in comparison to observations and that, in CORR, the location of maximum sea surface temperature (SST) variability associated with the AMV is found to the south of Greenland in a region where, in CTRL, the SST variability shows a local minimum. Furthermore, in CORR in the warm phase of the AMV, heat is released by the ocean to the atmosphere in the northwestern part of the Atlantic on decadal time scales, consistent with the dataset derived by *Gulev et al.* [2013] from observations, and absorbed by the ocean from the atmosphere to the west of the Europe and in parts of the tropics, leading to a basin wide response. *Brown et al.* [2016] have noted the importance of cloud feedback, both for amplifying the AMV signature in the northwestern Atlantic and for determining the atmosphere/ocean heat transfer in the tropics [see also *Yuan et al.*, 2016], a process we also think operates in our model. Here, we have argued that advection of heat by the mid-latitude westerlies also plays a role in heating the ocean to the west of Europe in the warm phase.

We have also used CORR to look at the modulation of the atmosphere/ocean heat flux on interdecadal time scales due to the low frequency variability of the atmospheric circulation, as seems to be a feature of the observed record during boreal winter [*Yamamoto and Palter*, 2016]. The results largely confirm the finding of *Yamamoto and Palter* [2016] that there can be multidecadal episodes in which more heat is removed from parts of the subpolar North Atlantic in the cold phase of the AMV than in the warm phase, contrast-

ing the picture when a long time series of the AMV is considered. This raises questions about the interpretation of the AMV and its impact on the atmosphere from the short observational data record, at least in subpolar regions where the atmosphere exhibits considerable internal variability. We also show that in CORR, the correct simulation of the AMV almost certainly requires changes in ocean heat transport, countering the suggestion made by *Clement et al.* [2015] that the AMV is driven locally by heat fluxes from the atmosphere without the need to invoke changes in ocean heat transport [see also *O'Reilly et al.*, 2016].

Finally, we note that although higher resolution models become more and more available, the representation of the North Atlantic Current and the cold bias do not necessarily improve with higher resolution (*Delworth et al.* [2012]; but see *Menary et al.* [2015]). The correction technique explored here is therefore a computationally inexpensive and pragmatic means to improve the flow field in the North Atlantic in models, thereby alleviating the cold bias, with the potential for significant improvement in the simulation of the overlying atmospheric circulation [*Scaife et al.*, 2011; *Keeley et al.*, 2012] and in the seasonal to decadal forecast skill in the Euro-Atlantic sector [*Scaife et al.*, 2014]. It should nevertheless be noted that it is not certain how ocean circulation will evolve with climate change in the future and that use of present-day climatological data to correct a model, as we have done here, might be inappropriate for future climate simulations.

Acknowledgments. AD is grateful for support through the Helmholtz Graduate School HOSST and the GEOMAR Helmholtz Centre for Ocean Research Kiel. Support is also acknowledged from the German Ministry for Education and Research (BMBF)

through MiKlip2, subproject 01LP1517D (ATMOS-MODINI). RJG is grateful for continuing support from GEOMAR. Data shown in this paper are available by email from Annika Drews (adrews@geomar.de).

Notes

1. This is the reason for using a 5 year low pass filter. This removes the interannual variability but preserves the decadal variability in CTRL.

References

Ba, J., N. S. Keenlyside, M. Latif, W. Park, H. Ding, K. Lohmann, J. Mignot, M. Menary, O. H. Otterå, B. Wouters, D. Salas y Mélia, A. Oka, A. Bellucci, and E. Volodin (2014), A multi-model comparison of Atlantic multidecadal variability, *Clim Dyn*, pp. 1–16, doi: 10.1007/s00382-014-2056-1.

Booth, B. B. B., N. J. Dunstone, P. R. Halloran, T. Andrews, and N. Bellouin (2012), Aerosols implicated as a prime driver of twentieth-century North Atlantic climate variability, *Nature*, *484*(7393), 228–232, doi:10.1038/nature10946.

Brown, P. T., M. S. Lozier, R. Zhang, and W. Li (2016), The necessity of cloud feedback for a basin-scale Atlantic Multidecadal Oscillation, *Geophys. Res. Lett.*, *43*(8), 2016GL068,303, doi:10.1002/2016GL068303.

Chylek, P., C. K. Folland, G. Lesins, M. K. Dubey, and M. Wang (2009), Arctic air temperature change amplification and the Atlantic Multidecadal Oscillation, *Geophys. Res. Lett.*, *36*(14), L14,801, doi:10.1029/2009GL038777.

Clement, A., K. Bellomo, L. N. Murphy, M. A. Cane, T. Mauritsen, G. Rädel, and B. Stevens (2015), The Atlantic Multidecadal Oscillation without a role for ocean cir-

culation, *Science*, *350*(6258), 320–324, doi:10.1126/science.aab3980.

Delworth, T. L., A. Rosati, W. Anderson, A. J. Adcroft, V. Balaji, R. Benson, K. Dixon, S. M. Griffies, H.-C. Lee, R. C. Pacanowski, G. A. Vecchi, A. T. Wittenberg, F. Zeng, and R. Zhang (2012), Simulated Climate and Climate Change in the GFDL CM2.5 High-Resolution Coupled Climate Model, *J. Climate*, *25*(8), 2755–2781, doi:10.1175/JCLI-D-11-00316.1.

Dima, M., and G. Lohmann (2007), A Hemispheric Mechanism for the Atlantic Multidecadal Oscillation, *J. Climate*, *20*(11), 2706–2719, doi:10.1175/JCLI4174.1.

Drews, A., R. J. Greatbatch, H. Ding, M. Latif, and W. Park (2015), The use of a flow field correction technique for alleviating the North Atlantic cold bias with application to the Kiel Climate Model, *Ocean Dynamics*, *65*(8), 1079–1093, doi:10.1007/s10236-015-0853-7.

Ebisuzaki, W. (1997), A Method to Estimate the Statistical Significance of a Correlation When the Data Are Serially Correlated, *J. Climate*, *10*(9), 2147–2153, doi:10.1175/1520-0442(1997)010¡2147:AMTETS¿2.0.CO;2.

Enfield, D. B., A. M. Mestas-Nuñez, and P. J. Trimble (2001), The Atlantic Multidecadal Oscillation and its relation to rainfall and river flows in the continental U.S., *Geophys. Res. Lett.*, *28*(10), 2077–2080, doi:10.1029/2000GL012745.

Flato, G., J. Marotzke, B. Abiodun, P. Braconnot, S. Chou, W. Collins, P. Cox, F. Driouech, S. Emori, V. Eyring, C. Forest, P. Gleckler, E. Guilyardi, C. Jakob, V. Kattsov, C. Reason, and M. Rummukainen (2014), Evaluation of Climate Models, in *Climate Change 2013 - The Physical Science Basis. Contribution of Working Group I to the*

Fifth Assess - ment Report of the Intergovernmental Panel on Climate Change, pp. 741–866, Cambridge University Press.

Folland, C. K., T. N. Palmer, and D. E. Parker (1986), Sahel rainfall and worldwide sea temperatures, 190185, *Nature*, *320*(6063), 602–607, doi:10.1038/320602a0.

Goldenberg, S. B., C. W. Landsea, A. M. Mestas-Nuñez, and W. M. Gray (2001), The Recent Increase in Atlantic Hurricane Activity: Causes and Implications, *Science*, *293*(5529), 474–479, doi:10.1126/science.1060040.

Gulev, S. K., M. Latif, N. Keenlyside, W. Park, and K. P. Koltermann (2013), North Atlantic Ocean control on surface heat flux on multidecadal timescales, *Nature*, *499*(7459), 464–467, doi:10.1038/nature12268.

Hurrell, J. W. (1995), Decadal Trends in the North Atlantic Oscillation: Regional Temperatures and Precipitation, *Science*, *269*(5224), 676–679, doi:10.1126/science.269.5224.676.

Kayano, M. T., and V. B. Capistrano (2014), How the Atlantic multidecadal oscillation (AMO) modifies the ENSO influence on the South American rainfall, *Int. J. Climatol.*, *34*(1), 162–178, doi:10.1002/joc.3674.

Keeley, S. P. E., R. T. Sutton, and L. C. Shaffrey (2012), The impact of North Atlantic sea surface temperature errors on the simulation of North Atlantic European region climate, *Q.J.R. Meteorol. Soc.*, *138*(668), 1774–1783, doi:10.1002/qj.1912.

Knight, J. R., R. J. Allan, C. K. Folland, M. Vellinga, and M. E. Mann (2005), A signature of persistent natural thermohaline circulation cycles in observed climate, *Geophys. Res. Lett.*, *32*(20), L20,708, doi:10.1029/2005GL024233.

Latif, M., and N. S. Keenlyside (2011), A perspective on decadal climate variability and predictability, *Deep Sea Research Part II: Topical Studies in Oceanography*, *58*(1718), 1880–1894, doi:10.1016/j.dsr2.2010.10.066.

Latif, M., E. Roeckner, M. Botzet, M. Esch, H. Haak, S. Hagemann, J. Jungclaus, S. Legutke, S. Marsland, U. Mikolajewicz, and J. Mitchell (2004), Reconstructing, Monitoring, and Predicting Multidecadal-Scale Changes in the North Atlantic Thermohaline Circulation with Sea Surface Temperature, *J. Climate*, *17*(7), 1605–1614, doi:10.1175/1520-0442(2004)017¡1605:RMAPMC¿2.0.CO;2.

Lazier, J. R. N. (1994), Observations in the Northwest Corner of the North Atlantic Current, *J. Phys. Oceanogr.*, *24*(7), 1449–1463, doi:10.1175/1520-0485(1994)024¡1449:OITNCO¿2.0.CO;2.

Madec, G. (2008), *NEMO ocean engine*, Note du Pôle de modélisation, Institut Pierre-Simon Laplace (IPSL), France.

McCabe, G. J., M. A. Palecki, and J. L. Betancourt (2004), Pacific and Atlantic Ocean influences on multidecadal drought frequency in the United States, *PNAS*, *101*(12), 4136–4141, doi:10.1073/pnas.0306738101.

McCarthy, G. D., I. D. Haigh, J. J.-M. Hirschi, J. P. Grist, and D. A. Smeed (2015), Ocean impact on decadal Atlantic climate variability revealed by sea-level observations, *Nature*, *521*(7553), 508–510, doi:10.1038/nature14491.

Menary, M. B., D. L. R. Hodson, J. I. Robson, R. T. Sutton, R. A. Wood, and J. A. Hunt (2015), Exploring the impact of CMIP5 model biases on the simulation of North Atlantic decadal variability, *Geophys. Res. Lett.*, *42*(14), 2015GL064,360, doi:

10.1002/2015GL064360.

O'Reilly, C. H., M. Huber, T. Woollings, and L. Zanna (2016), The signature of low-frequency oceanic forcing in the Atlantic Multidecadal Oscillation, *Geophys. Res. Lett.*, p. 2016GL067925, doi:10.1002/2016GL067925.

Otterå, O. H., M. Bentsen, H. Drange, and L. Suo (2010), External forcing as a metronome for Atlantic multidecadal variability, *Nature Geosci*, *3*(10), 688–694, doi:10.1038/ngeo955.

Park, W., N. Keenlyside, M. Latif, A. Ströh, R. Redler, E. Roeckner, and G. Madec (2009), Tropical Pacific Climate and Its Response to Global Warming in the Kiel Climate Model, *J. Climate*, *22*(1), 71–92, doi:10.1175/2008JCLI2261.1.

Rayner, N. A., D. E. Parker, E. B. Horton, C. K. Folland, L. V. Alexander, D. P. Rowell, E. C. Kent, and A. Kaplan (2003), Global analyses of sea surface temperature, sea ice, and night marine air temperature since the late nineteenth century, *J. Geophys. Res.*, *108*(D14), 4407, doi:10.1029/2002JD002670.

Roeckner, E., G. Baeuml, L. Bonaventura, R. Brokopf, M. Esch, M. Giorgetta, S. Hagemann, I. Kirchner, L. Kornblueh, E. Manzini, A. Rhodin, U. Schlese, U. Schulzweida, and A. Tompkins (2003), The atmospheric general circulation model ECHAM5 - Part 1, *MPI-Report 349*, Max Planck Institute for Meteorology, Hamburg, Gemany.

Scaife, A. A., D. Copsey, C. Gordon, C. Harris, T. Hinton, S. Keeley, A. O'Neill, M. Roberts, and K. Williams (2011), Improved Atlantic winter blocking in a climate model, *Geophys. Res. Lett.*, *38*(23), L23,703, doi:10.1029/2011GL049573.

Scaife, A. A., A. Arribas, E. Blockley, A. Brookshaw, R. T. Clark, N. Dunstone, R. Eade, D. Fereday, C. K. Folland, M. Gordon, L. Hermanson, J. R. Knight, D. J. Lea, C. MacLachlan, A. Maidens, M. Martin, A. K. Peterson, D. Smith, M. Vellinga, E. Wallace, J. Waters, and A. Williams (2014), Skillful long-range prediction of European and North American winters, *Geophys. Res. Lett.*, *41*(7), 2014GL059,637, doi: 10.1002/2014GL059637.

Schlesinger, M. E., and N. Ramankutty (1994), An oscillation in the global climate system of period 65-70 years, *Nature*, *367*(6465), 723–726, doi:10.1038/367723a0.

Steinman, B. A., M. E. Mann, and S. K. Miller (2015), Atlantic and Pacific multidecadal oscillations and Northern Hemisphere temperatures, *Science*, *347*(6225), 988–991, doi: 10.1126/science.1257856.

Sutton, R. T., and D. L. R. Hodson (2005), Atlantic Ocean Forcing of North American and European Summer Climate, *Science*, *309*(5731), 115–118, doi:10.1126/science.1109496.

Tandon, N. F., and P. J. Kushner (2015), Does External Forcing Interfere with the AMOC's Influence on North Atlantic Sea Surface Temperature ?, *J. Climate*, doi: 10.1175/JCLI-D-14-00664.1.

Ting, M., Y. Kushnir, R. Seager, and C. Li (2009), Forced and Internal Twentieth-Century SST Trends in the North Atlantic, *J. Climate*, *22*(6), 1469–1481, doi: 10.1175/2008JCLI2561.1.

Valcke, S. (2006), OASIS3 User Guide. PRISM technical report., *Tech. Rep. TR/CMGC/06/73*, CERFACS, Toulouse, France.

Valcke, S. (2013), The OASIS3 coupler: a European climate modelling community software, *Geosci. Model Dev.*, *6*(2), 373–388, doi:10.5194/gmd-6-373-2013.

Wang, C., L. Zhang, S.-K. Lee, L. Wu, and C. R. Mechoso (2014), A global perspective on CMIP5 climate model biases, *Nature Clim. Change*, *4*(3), 201–205, doi:10.1038/nclimate2118.

Yamamoto, A., and J. B. Palter (2016), The absence of an Atlantic imprint on the multidecadal variability of wintertime European temperature, *Nat Commun*, *7*, 10,930, doi:10.1038/ncomms10930.

Yuan, T., L. Oreopoulos, M. Zelinka, H. Yu, J. R. Norris, M. Chin, S. Platnick, and K. Meyer (2016), Positive low cloud and dust feedbacks amplify tropical North Atlantic Multidecadal Oscillation, *Geophys. Res. Lett.*, *43*(3), 2016GL067,679, doi:10.1002/2016GL067679.

Zhang, R., and T. L. Delworth (2006), Impact of Atlantic multidecadal oscillations on India/Sahel rainfall and Atlantic hurricanes, *Geophys. Res. Lett.*, *33*(17), L17,712, doi:10.1029/2006GL026267.

Zhang, R., T. L. Delworth, R. Sutton, D. L. R. Hodson, K. W. Dixon, I. M. Held, Y. Kushnir, J. Marshall, Y. Ming, R. Msadek, J. Robson, A. J. Rosati, M. Ting, and G. A. Vecchi (2013), Have Aerosols Caused the Observed Atlantic Multidecadal Variability?, *J. Atmos. Sci.*, *70*(4), 1135–1144, doi:10.1175/JAS-D-12-0331.1.

Figure 1. Time series of the AMV (a) in observations (OBS; HadISST 1900-2012), (b) the uncorrected model (CTRL), and (c) the corrected model (CORR). All time series have been 5 year low pass filtered. The bar in (c) marks the 70 year long episode discussed in the text and used in Fig. 4a.

Figure 2. The spatial pattern of SST varability associated with the AMV in (a) observations, (b) CTRL, and (c) CORR. Shown are regressions of 5 year low pass filtered SST ((a) HadISST 1900-2012, (b) and (c) 700 model years) onto the corresponding 5 year low pass filtered AMV index. Units are °C/°C. Areas with more than 15% mean sea ice in March have been masked. Longitude/latitude intervals are 15° in all figures. For the same figure, but using AMV indices normalized by their standard deviation, see Fig. S9.

Figure 3. Regression of the annual mean turbulent (i.e. sensible and latent) surface heat flux (positive upward) on the AMV index: (a) CTRL, (b) CORR, and (c) the dataset produced by *Gulev et al.* [2013] (1900-2007). For the models, time series are 5 year low pass filtered; in (c) time series are smoothed with an 11 year running mean (cf. *Gulev et al.* [2013]). Units are $\mathrm{Wm^{-2}K^{-1}}$. Areas with more than 15% mean sea ice cover in March are masked (HadISST used for the observed estimate of the AMV index and sea ice in (c)). Hatching denotes that the corresponding correlation coefficients are significantly different from zero at the 95% or greater level according to the method of *Ebisuzaki* [1997].

Figure 4. Regression of the winter (DJF) mean turbulent surface heat flux (positive upward) on the winter (DJF) AMV index from CORR for (a) the years 620-689, which exhibit anti-correlated NAO and AMV indices, and (b) the whole 700 years of model data. All time series are 5 year low pass filtered. Units are $Wm^{-2}K^{-1}$. Areas with more than 15% mean sea ice cover in March are masked. Hatching combined with white stippling denotes areas with correlations that are significantly different from zero at the 95 % level using the method of *Ebisuzaki* [1997].

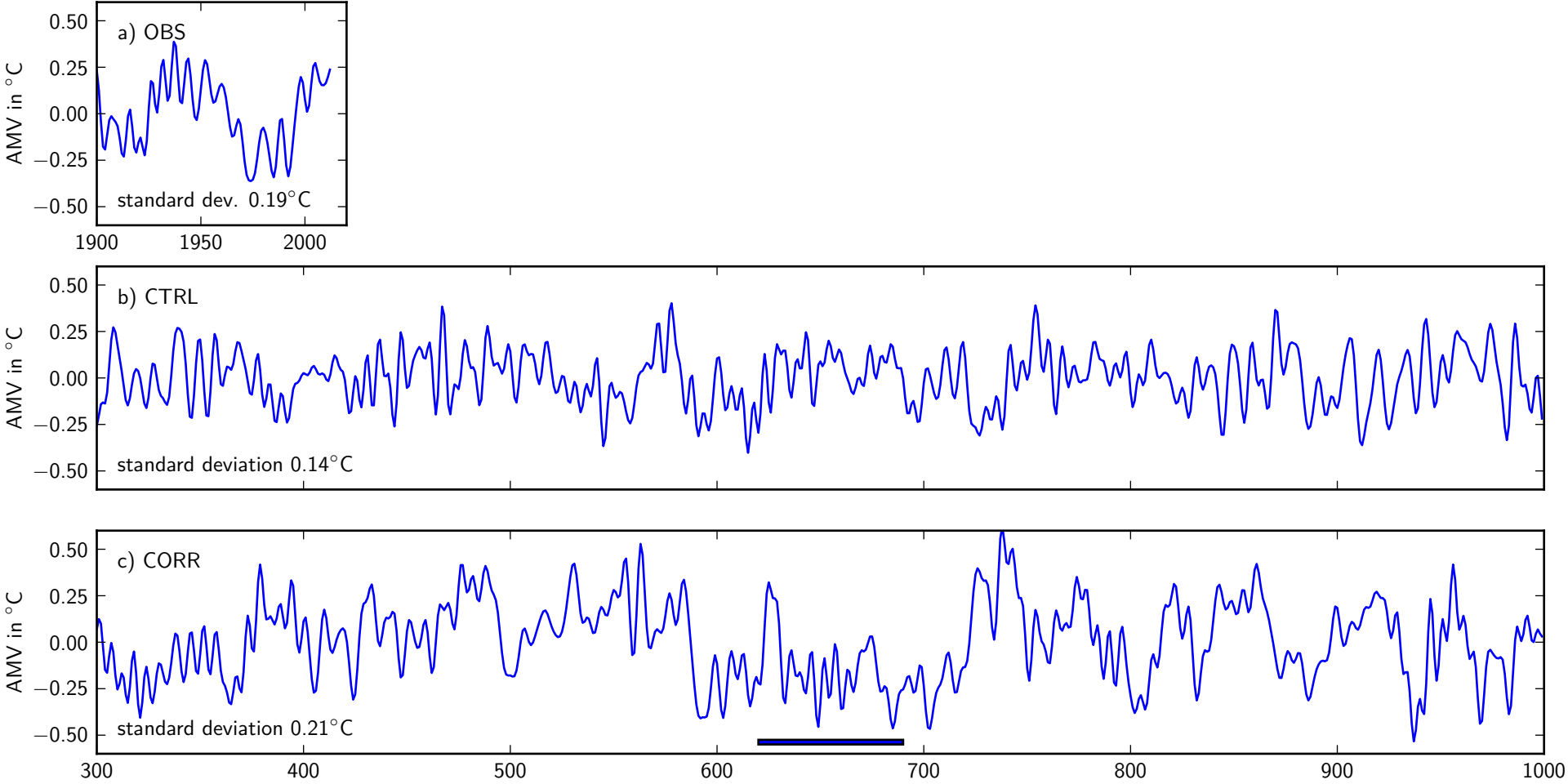
a) OBS
standard dev. 0.19°C
b) CTRL
standard deviation 0.14°C
c) CORR
standard deviation 0.21°C
AMV in °C
0.50
0.25
0.00
−0.25
−0.50
1900
1950
2000
300
400
500
600
700
800
900
1000

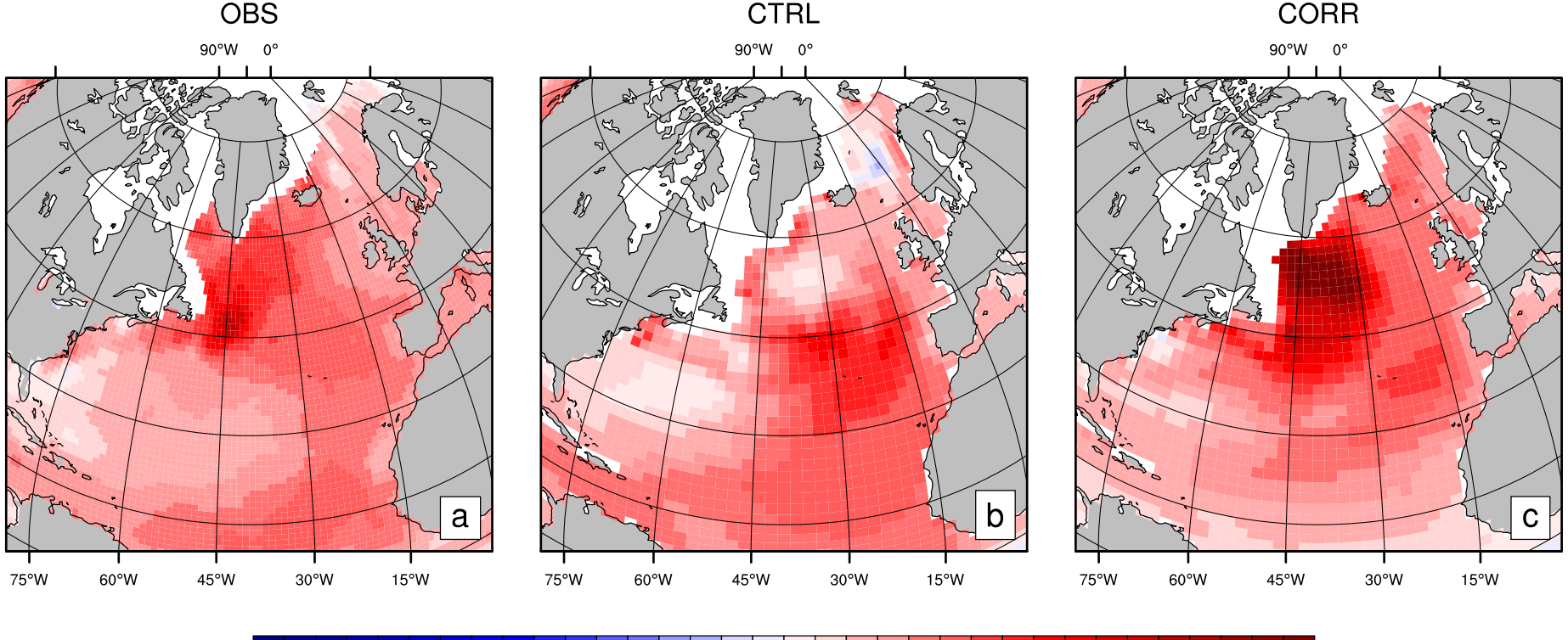
OBS
CTRL
CORR
90°W
0°
75°W
60°W
45°W
30°W
15°W
a
b
c
-4
-3.5
-3
-2.5
-2
-1.5
-1
-.5
0
.5
1
1.5
2
2.5
3
3.5
4

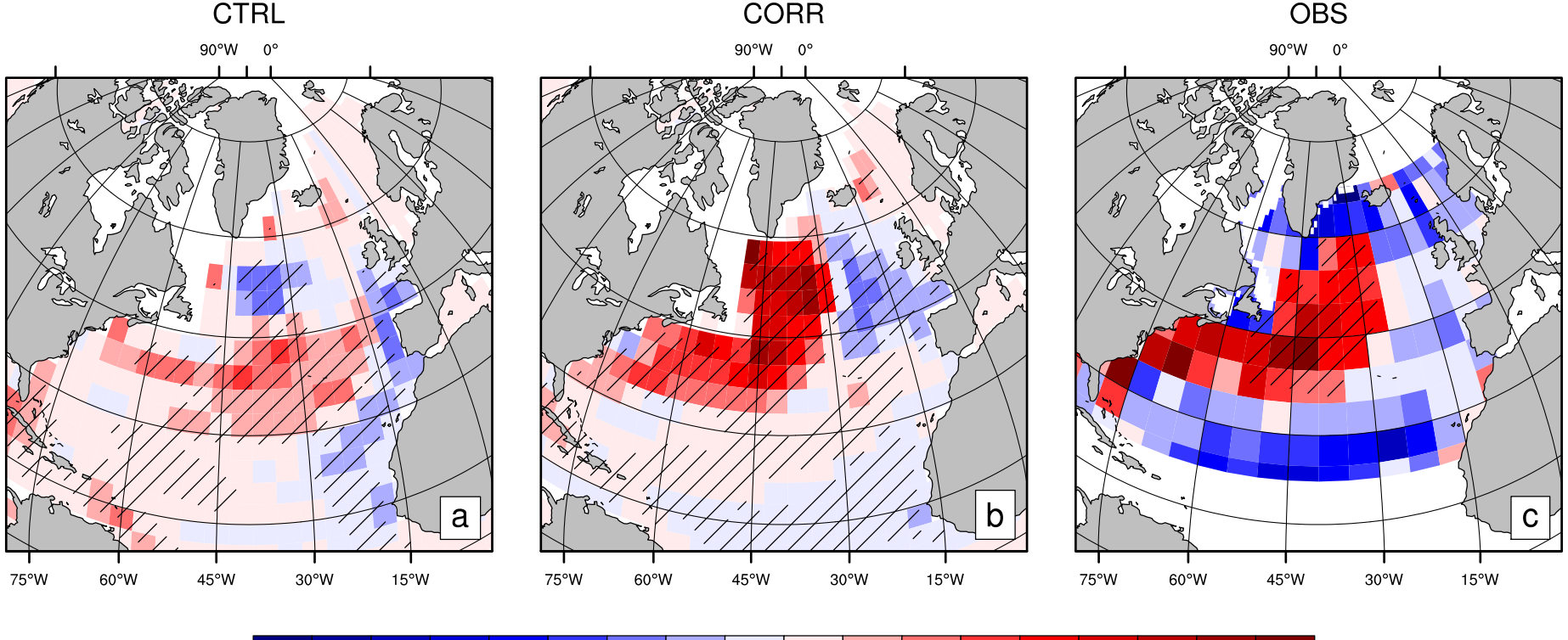
CTRL
CORR
OBS
90°W
0°
75°W
60°W
45°W
30°W
15°W
a
b
c
-40 -35 -30 -25 -20 -15 -10 -5 0 5 10 15 20 25 30 35 40

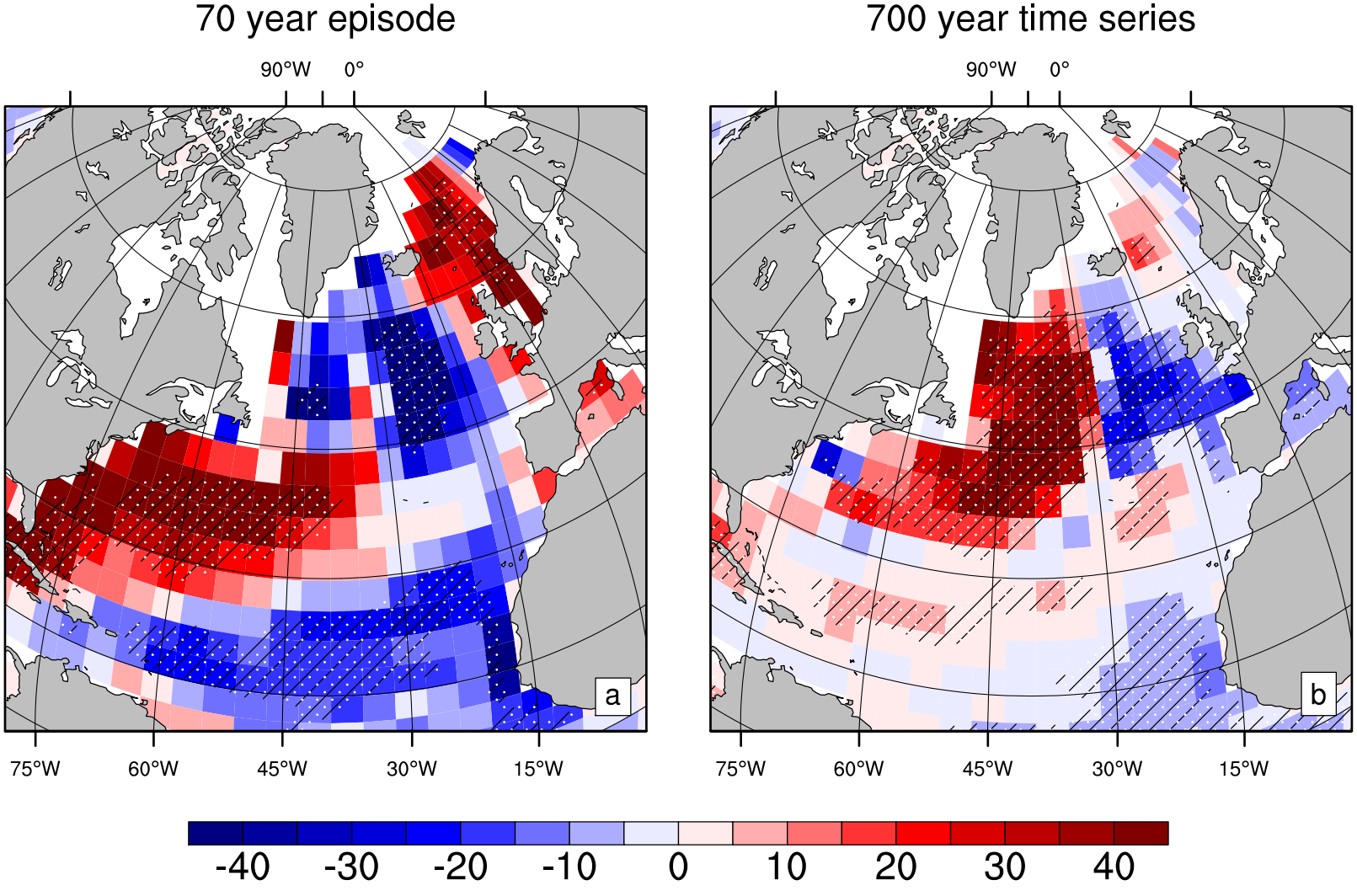
70 year episode
700 year time series
90°W
0°
75°W
60°W
45°W
30°W
15°W
a
b
-40
-30
-20
-10
0
10
20
30
40